communications biology

Article

https://doi.org/10.1038/s42003-024-07070-z

Precision-cut liver slices as an ex vivo model to assess impaired hepatic glucose production

Ligia Akemi Kiyuna[1,6], Kishore Alagere Krishnamurthy[1,6], Esther B. Homan[1], Miriam Langelaar-Makkinje[1], Albert Gerding[1,2], Trijnie Bos[2], Dorenda Oosterhuis[3], Ruben J. Overduin[1,4], Andrea B. Schreuder[1,4], Vincent E. de Meijer[5], Peter Olinga[3], Terry G. J. Derks[1,4], Karen van Eunen[1], Barbara M. Bakker[1,7] ✉ & Maaike H. Oosterveer[1,2,7] ✉

Fasting hypoglycemia is a severe and incompletely understood symptom of various inborn errors of metabolism (IEM). Precision-cut liver slices (PCLS) represent a promising model for studying glucose production ex vivo. This study quantified the net glucose production of human and murine PCLS in the presence of different gluconeogenic precursors. Dihydroxyacetone-supplemented slices from the fed mice yielded the highest rate, further stimulated by forskolin and dibutyryl-cAMP. Moreover, using ^{13}C isotope tracing, we assessed the contribution of glycogenolysis and gluconeogenesis to net glucose production over time. Pharmacological inhibition of the glucose 6-phosphate transporter SLC37A4 markedly reduced net glucose production and increased lactate secretion and glycogen storage, while glucose production was completely abolished in PCLS from glycogen storage disease type Ia and Ib patients. In conclusion, this study identifies PCLS as an effective ex vivo model to study hepatic glucose production and opens opportunities for its future application in IEM research and beyond.

Inborn errors of metabolism (IEM) constitute a heterogeneous group of disorders characterized by impairments in metabolic pathways, which drive a range of clinical manifestations with different degrees of severity (e.g., exercise intolerance, muscle, and abdominal pain, seizures) and can be associated with high mortality[1]. Although individually rare, altogether, IEMs are estimated to have a prevalence of 1:2000 live births worldwide[2]. To date, more than 1.000 IEMs have been reported[3,4]. The disorders can be broadly divided into three main groups: (I) intoxication disorders, e.g., aminoacidopathies, (II) energy metabolism disorders, e.g., fatty acid oxidation disorders/FAOD, and (III) storage diseases, e.g., glycogen storage diseases/GSDs[1]. Several IEMs present with loss of glucose homeostasis, which in turn can cause acute and life-threatening symptoms (e.g., fasting hypoglycemia), and drive chronic illness throughout life[5–7]. Despite its severity, the mechanisms underlying dysfunctional glucose production in several IEMs remain incompletely understood.

The liver is the central metabolic hub of the body and maintains glucose homeostasis under various conditions. After a meal, the liver takes up the excess circulating glucose and stores it as glycogen, which serves as a glucose reservoir through fasting periods. In the post-absorptive state, the liver contributes up to 80–90% of the endogenous glucose production[8]. Besides glycogenolysis, during prolonged fasting the liver synthesizes glucose de novo from endogenous substrates (e.g., glycerol, lactate) at the expense of ATP, in a process referred to as gluconeogenesis. Hepatic glucose production is tightly regulated by hormones, neural stimulation, and sensitive to intracellular/extracellular nutrient concentrations[9]. The intrinsic complexity of hepatic physiology as well as the contribution of intestine and kidney to endogenous glucose production[10,11] make it challenging to isolate and study the liver's contribution to systemic glucose (un)balance in vivo. In this context, liver-specific in vitro/ex vivo models are critical to unravel the biochemical and molecular mechanisms underlying dysfunctional hepatic glucose production.

Historically, different hepatic model systems have been used to assess glucose production in vivo[12], in vitro (primary hepatocytes, cell lines)[13,14] and ex vivo (perfused liver or precision-cut liver slices (PCLS)[15,16]. As early as the

[1]Department of Pediatrics, University of Groningen, University Medical Center Groningen, Groningen, The Netherlands. [2]Department of Laboratory Medicine, University of Groningen, University Medical Center Groningen, Groningen, The Netherlands. [3]Department of Pharmaceutical Technology and Biopharmacy, University of Groningen, Groningen, The Netherlands. [4]Department of Metabolic Diseases, Beatrix Children's Hospital, University of Groningen, University Medical Center Groningen, Groningen, The Netherlands. [5]Section of HPB Surgery and Liver Transplantation, Department of Surgery, University of Groningen, University Medical Center Groningen, Groningen, The Netherlands. [6]These authors contributed equally: Ligia Akemi Kiyuna, Kishore Alagere Krishnamurthy. [7]These authors jointly supervised this work: Barbara M. Bakker, Maaike H. Oosterveer. ✉e-mail: b.m.bakker01@umcg.nl; moosterveer@hotmail.com

1960s, perfused rat livers were used to study gluconeogenesis ex vivo[16]. Despite the advantages of working with the intact organ, this model is non-economical, and does not allow high-throughput experimentation. Isolated or primary hepatocytes are the gold standard in vitro liver cell models. Liver-derived cell lines, such as HepG2 and IHH cells, are relatively cheap to culture, easy to multiply and are often used to study hepatic metabolism[17]. Yet, these cell lines exhibit low levels of glucose 6-phosphatase (the enzyme that produced glucose), and therefore low net glucose production rates[18]. Primary hepatocytes derived from murine and human livers are preferred models to study hepatic glucose production in vitro, as they show a higher production rate than cell lines. However, net glucose production rates of primary hepatocytes are still considerably lower than endogenous glucose production rates quantified in vivo (Table 1).

One asset of PCLS is that this model system comprises all the different hepatic cell types and conserves tissue structure, in which the hepatocytes are embedded in their original microenvironment. Therefore, PCLS more closely resemble in vivo conditions than other cell-based models that exclusively contain hepatocytes. Although previous studies have demonstrated that PCLS show net glucose production in the initial hours of culture[15], to the best of our knowledge, quantitative measures of PCLS glucose production rates have not been reported yet. Moreover, loss of hepatic glucose production can be caused by an impairment in glycogenolysis and/or gluconeogenesis while the contribution of these individual processes to hepatic glucose production have not been systematically assessed in PCLS. Furthermore, experimental conditions such as the medium composition/gluconeogenic precursor supply, use of hormonal or pharmacological stimuli, and incubation times, may impact on glucose production rates[15]. As specific experimental conditions may favor the study of either glycogenolysis or gluconeogenesis, insight into glucose production rates under well-defined experimental conditions is essential when designing a study that aims to investigate dysfunctional hepatic glucose production in specific disease contexts. Altogether, a comprehensive characterization of PCLS glucose production in the context of human disease is warranted.

The current study therefore aims to optimize culture conditions and comprehensively characterize PCLS as an experimental model to investigate (dys)functional glucose production in the context of metabolic disease by (1) systematically assessing the effect of different gluconeogenic precursors on net glucose production rates of PCLS derived from fed and fasted mice and human liver; (2) estimating the fractional contributions of gluconeogenesis and glycogenolysis to PCLS glucose production; (3) evaluating the effect of hormonal and pharmacological stimulation on net glucose production rates; and (4) providing a proof-of-concept for the use of PCLS to investigate hepatic glucose production in IEM, specifically hepatic GSD type Ia and Ib.

Results

Murine PCLS produce glucose ex vivo and DHA supplementation leads to a higher net glucose production rate

We first confirmed that murine PCLS produces glucose ex vivo and optimized the experimental conditions to this end. In vivo, endogenous glucose production is activated during fasting. As blood glucose levels drop, the liver degrades its glycogen stores and synthesizes glucose de novo from various gluconeogenic substrates (Fig. 1a)[19]. To stimulate glucose production ex vivo, PCLS derived from either fed or overnight fasted mice were incubated in glucose-free Williams E (WE) medium, either without gluconeogenic precursors, or supplemented with dihydroxyacetone (DHA), lactate/pyruvate mixture (L/P), or glycerol (Fig. 1a, b).

PCLS derived from both fed and fasted mice produced glucose in the presence and absence of gluconeogenic precursors (Fig. 1c, d and Supplementary Table S2). The glucose levels measured in PCLS medium represent the net result of production and consumption. In fed mice, DHA supplementation showed an increased rate of net glucose production measured over 5 h (Fig. 1e) and an increased net cumulative glucose level over 24 h (Fig. 1f). In PCLS from fasted mice, the response to DHA was ablated: neither the net glucose production rate nor the 24 h net cumulative glucose level was affected by precursor supplementation (Fig. 1e, f).

Primary hepatocytes, a commonly used in vitro model to study hepatic glucose production, are often subjected to a 24 h-recovery period in high-glucose medium after isolation[20]. To test how such a recovery period would affect the viability and glucose production of PCLS, they were pre-incubated in WE medium containing 11 mM glucose for 24 h prior to incubation in the glucose-free medium (Fig. 1b, g–j). Slice viability was preserved during pre-incubation (Supplementary Table S3). Over the first 5 h of incubation in glucose-free medium, both the net cumulative glucose values and the glucose production rates were lower than in PCLS that were not pre-incubated (Fig. 1g–i and Supplementary Table S2). Interestingly, after 24 h in culture, the pre-incubated PCLS exhibited the same glucose production pattern as those without the pre-incubation, albeit at lower absolute values (cf. Fig. 1f, j). Also after pre-incubation, DHA supplementation resulted in both the highest net glucose production rates and the highest net cumulative glucose levels in pre-incubated PCLS from fed mice (Fig. 1i, j).

In summary, the net ex vivo glucose production rates by murine PCLS depend on the availability and type of gluconeogenic substrate, as well as on the feeding state of the mice. Since the highest net glucose production rates were observed with DHA as the precursor, all further experiments were done with PCLS supplemented with either NP or DHA. Since the pre-incubation in a high-glucose medium did not enhance glucose production, it was discontinued.

Table 1 | Estimates of glucose production rates in vivo and in vitro

System	Source	Gluconeogenic substrate	Glucose production rate (nmol/mg liver protein/h)
Mouse	In vivo	–	1667[33,34a]
Human	In vivo	–	234[74a]
AML12 cells	Mouse	Lactate/pyruvate (20 mM/2 mM)	45[13]
HEPG2 cells	Human	Lactate/pyruvate (20 mM/2 mM)	75[13]
PH5CH8 cells	Human	Lactate/pyruvate (20 mM/2 mM)	80[13]
IHH cells	Human	Lactate/pyruvate (20 mM/2 mM)	120[13]
Primary hepatocytes	Mouse	Pyruvate (1 mM)	140[14]
Primary hepatocytes	Mouse	Lactate/pyruvate (20 mM/2 mM)	280[13]
Primary hepatocytes	Mouse	Dihydroxyacetone-phosphate (2 mM)	290[14]
Primary hepatocytes	Mouse	Dihydroxyacetone (5 mM)	195[38]
Primary hepatocytes	Mouse	Glycerol (2 mM)	120[38]

[a]Refer to the calculation in Supplementary Table S1.

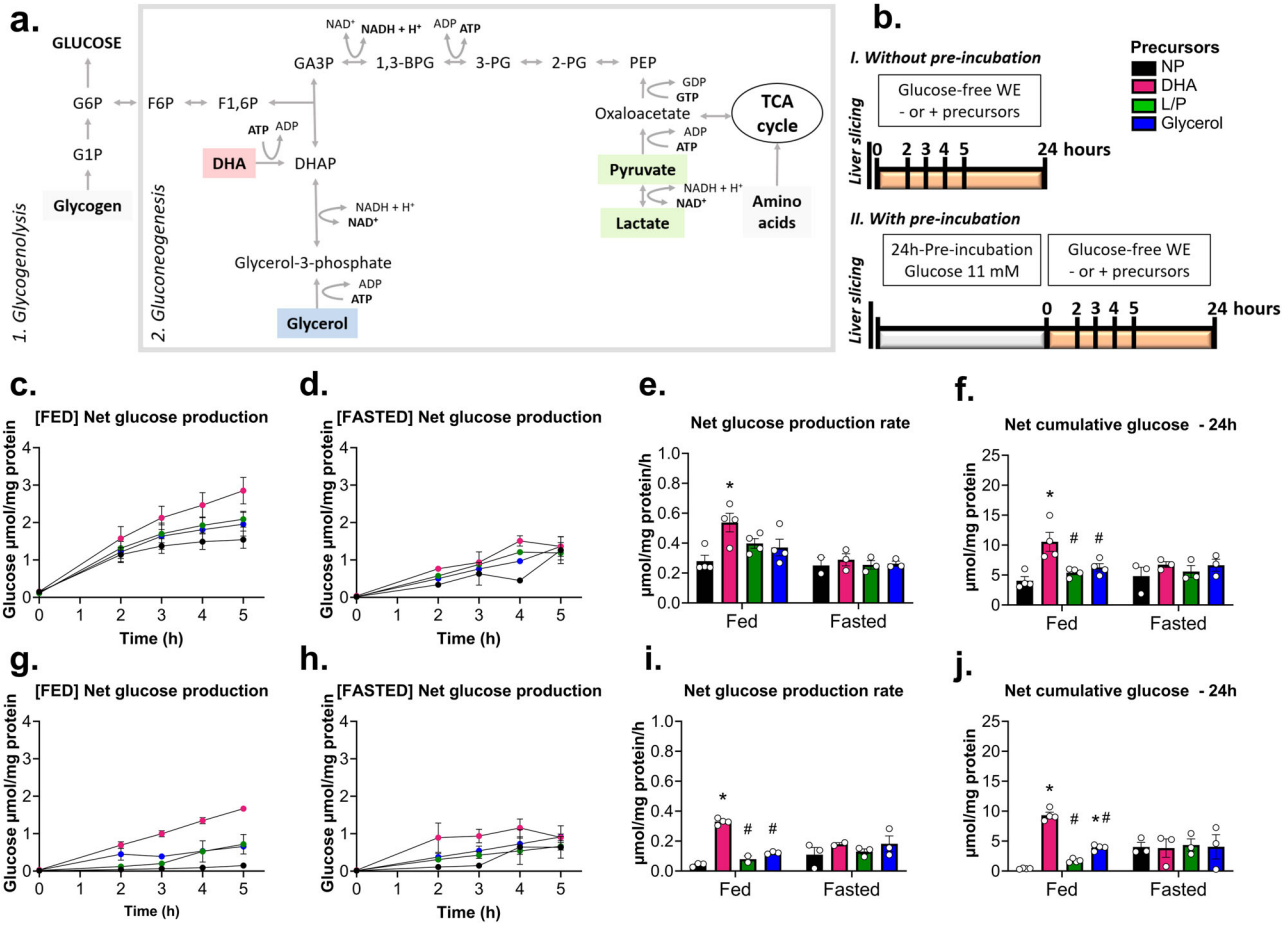

Fig. 1 | Glucose production. a Simplified scheme of the main glucose production pathways: 1. Glycogenolysis and 2. Gluconeogenesis; **b** Experimental design and conditions; NP no precursor, DHA dihydroxyacetone, L/P lactate/pyruvate; **c–f** Without 24 h pre-incubation: 5 h net cumulative glucose production of PCLS from fed (**c**) and fasted (**d**) mice; **e** Net glucose production rate of PCLS from fed and fasted mice; **f** 24 h net cumulative glucose of PCLS from fed and fasted mice; **g–j** With 24 h pre-incubation: 5 h net cumulative glucose production of PCLS from fed (**g**) and fasted (**h**) mice; **i** Net glucose production rate of PCLS from fed and fasted mice; **j** 24 h net cumulative glucose of PCLS from fed and fasted mice; $^{*}p < 0.05$, vs NP in the same condition; $^{\#}p < 0.05$, vs DHA group in the same condition; data presented as mean ± SEM; the individual data points are depicted in Supplementary Fig. S1; $n = 3–4$ mice per group.

Forskolin and dibutyryl-cAMP stimulate net glucose production

In vivo, hepatic glucose uptake, storage, and synthesis are modulated by hormones[19]. Glucagon activates glycogenolysis and gluconeogenesis (Fig. 2a)[21]. In contrast, insulin stimulates glycogen synthesis and inhibits gluconeogenesis, thereby decreasing net glucose production[22]. We tested if the PCLS responded to hormonal stimulation in a similar way. However, under the tested conditions, insulin and glucagon had no effect on the net cumulative glucose production by PCLS, irrespective of the feeding state of the mice (Fig. 2b, c and Supplementary Table S4).

Cyclic adenosine monophosphate (cAMP) is a ubiquitous second messenger, essential in the glucagon signaling cascade (Fig. 2a). In in vitro studies, forskolin and dibutyryl-cAMP are often used as glucagon mimetics[23,24]. Forskolin activates adenylate cyclase (AC), thus increasing cAMP, while dibutyryl-cAMP is a cell-permeable analog of cAMP (Fig. 2a). Notably, both forskolin and dibutyryl-cAMP increased the net glucose production by PCLS. In the absence of precursor, forskolin only had an effect in PCLS from fasted mice, while dibutyryl-cAMP augmented net glucose production in PCLS from both fed and fasted animals (Fig. 2b, c and Supplementary Table S4). A similar stimulating effect was observed in PCLS supplemented with DHA, albeit on the brink of significance (Fig. 2d), with the difference that forskolin now stimulated net glucose production in PCLS from fed, but not fasted mice. These results suggest that the signaling cascade downstream of the glucagon receptor is active in murine PCLS, as it responded to an increase in the cAMP pool.

Since glucagon and insulin did not affect net glucose production after 5 h incubation, we tested if these hormones activated their downstream signaling pathways in PCLS (Fig. 3). Indeed, insulin increased the phosphorylation of its downstream target Akt (Fig. 3a, c–e). Upregulation of the pAkt-T308/Akt ratio was sustained during 5 h. pAKT-T308 itself showed a transient peak at 30 min after administration of insulin, but remained elevated during the entire 5 h of the experiment. Nevertheless, insulin had no effect on glucose production, not even at the earlier time points (Fig. 3g). Glucagon induced a pronounced, transient phosphorylation of its downstream target, PKA substrates (Fig. 3b, f). In agreement with this, glucagon positively stimulated net glucose production (Fig. 3h), but not significantly ($p = 0.07$) and only transiently during the first 2 h. Finally, forskolin also induced phosphorylation of PKA substrates, however, an upregulation of net glucose production was not observed (Fig. 3i–k).

In conclusion, hormone signaling was intact in PCLS, but the downstream effect on glucose production was blunted in the case of insulin and transient in the case of glucagon.

Both glycogenolysis and gluconeogenesis contribute to glucose production by murine PCLS, and their relative contributions change over time

Next, we investigated the sources of glucose production by murine PCLS. Glycogenolysis and gluconeogenesis are the pathways responsible for endogenous glucose production (Fig. 1a). To estimate their relative

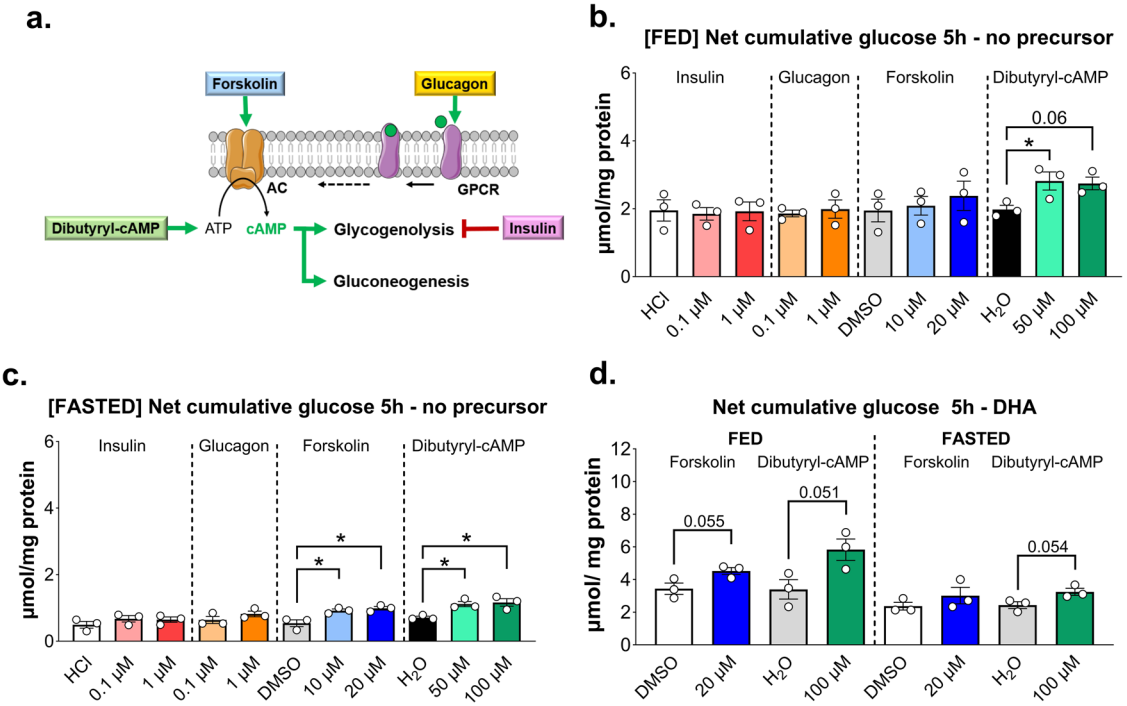

Fig. 2 | Effects of hormone stimulation on glucose production. a Simplified scheme of mechanism of action of insulin, glucagon, forskolin, and dibutyryl-cAMP; 5 h net cumulative glucose production of PCLS derived from fed (**b**) and fasted (**c**) mice incubated with WE medium without precursor treated with insulin, glucagon, forskolin or dibutyryl-cAMP; **d** 5 h net glucose production of PCLS derived from fed and fasted mice incubated with WE medium supplemented with DHA and treated with forskolin or dibutyryl-cAMP; HCl was used as a vehicle for insulin and glucagon, and DMSO was used as a vehicle for forskolin; $*p < 0.05$, vs the corresponding vehicle; data presented as mean ± SEM; $n = 3$ mice per group. GPCR G protein-coupled receptor, AC adenylate cyclase.

contributions, the culture medium was supplemented with the labeled gluconeogenic precursors [2-^{13}C]-glycerol or [2-^{13}C]-DHA. These precursors are first converted into [2-^{13}C]-dihydroxyacetone-phosphate (DHAP in Fig. 1a), which is in rapid equilibrium with glyceraldehyde 3-phosphate (G3P). In the following, we will denote DHAP and G3P together as the triose phosphate (TrioseP) pool. Glucose is formed from two molecules of TrioseP. Since there are other sources of TrioseP besides [2-^{13}C]-glycerol or [2-^{13}C]-DHA, only a fraction of the TrioseP pool contains the ^{13}C label. Theoretically, conversion of Triose-P to glucose could lead to the formation of glucose isotopologues containing no ^{13}C atoms (m + 0, formed from two molecules of unlabeled TrioseP), one ^{13}C atom, hence a mass unit heavier (m + 1, from a labeled and an unlabeled TrioseP), or two ^{13}C atoms (m + 2, from two labeled TrioseP). Indeed, we observed that incubation of PCLS with either [2-^{13}C]-glycerol or [2-^{13}C]-DHA led to ^{13}C incorporation into the produced glucose (Fig. 4a, b). This demonstrates that these precursors were utilized as substrates for gluconeogenesis.

The relative contributions of gluconeogenesis and glycogenolysis were subsequently calculated from the measured isotopologue distributions, as outlined in the section "Methods". Throughout the entire experiment, both gluconeogenesis and glycogenolysis contributed to the net cumulative glucose production, irrespective of which labeled substrate was given (Fig. 4c, d). Initially, approximately 70% of the net cumulative glucose originated from glycogen (Fig. 4c, d). After 5 h in culture, however, the glycogen stores were substantially and equally reduced in all conditions (Fig. 4e). In line with this, the contribution of glycogenolysis decreased over time, in favor of gluconeogenesis (Fig. 4c, d). The contribution of gluconeogenesis increased faster in [2-^{13}C]-DHA-supplemented medium than in the [2-^{13}C]-glycerol medium. After 24 h, gluconeogenesis was the main contributor to the net glucose produced in the medium supplemented with [2-^{13}C]-DHA (68.6 ± 1.9%), while in the medium with [2-^{13}C]-glycerol, gluconeogenesis contributed 54.3 ± 9.7% and glycogenolysis 45.7 ± 9.7% (Fig. 4c, d). The larger contribution of gluconeogenesis in the [2-^{13}C]-DHA medium is consistent with the higher net glucose production rate in the medium supplemented with DHA, compared to that supplemented with glycerol (Fig. 1).

Finally, the ratio of m + 1 over m + 2 glucose allowed us to calculate the fraction of labeled TrioseP (Fig. 4f and section "Methods"). The total precursor enrichment of the TrioseP pool (m + 1) was less than 100% after 24 h, specifically 85.8 ± 3.8% (DHA) and 80.5 ± 0.9% (glycerol). It indicates that the TrioseP pool was not only filled from [2-^{13}C]-glycerol or [2-^{13}C]-DHA, but also from other non-labeled sources. These could be for instance amino acids in the medium, which can be used by the liver as gluconeogenic precursors. Based on the calculated net glucose production rate and gluconeogenesis contribution (Supplementary Text 1), we estimated that 0.27 mM amino acid would be necessary from the medium over 24 h to supply the unlabeled TrioseP fraction. However, no substantial decrease of any amino acid was observed in the medium of the PCLS during the course of incubation (Table S5). In fact, after 24 h, we observed a significant increase in branched-chain amino acids in the medium of PCLS incubated without precursors. Glutamate was also elevated in the medium of PCLS incubated with no precursor and DHA.

Altogether, these results demonstrate that both glycogenolysis and gluconeogenesis take place in the PCLS. Their relative contributions to the net glucose production shift in time and in response to different gluconeogenic precursors.

S4048-treated murine PCLS mimic the disease phenotype of hepatic glycogen storage disease (GSD) type Ib ex vivo

Our goal was to characterize murine PCLS as an ex vivo model to study dysfunctional glucose production in metabolic disease. We selected GSD type Ib as a proof of concept, since it has a known genetic cause with a clear clinical phenotype, and its primary defect is impaired glucose production. GSD type Ib is caused by a loss-of-function mutation in the gene encoding the glucose 6-phosphate (G6P) transporter SLC37A4[25] (Fig. 5a). SLC37A4 transports G6P into the lumen of the endoplasmic reticulum, to where it is converted into free glucose by glucose 6-phosphatase (G6PC). In patients,

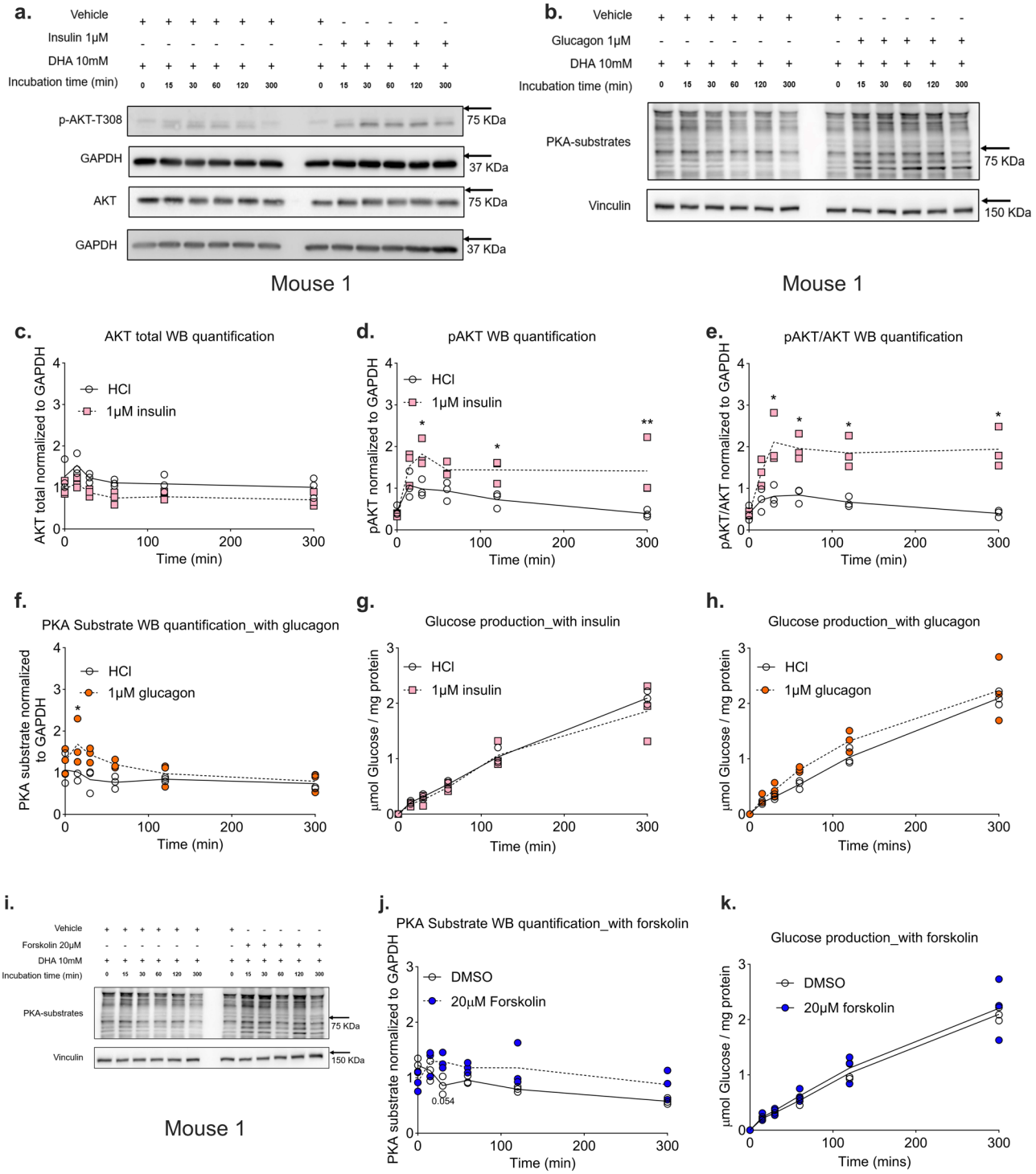

Fig. 3 | Time course of effects of insulin, glucagon and forskolin on downstream signaling pathways and net glucose production. Immunoblotting of PCLS derived from fed mice incubated with WE medium supplemented with DHA and treated with insulin (**a**) or glucagon (**b**) at different time points (0, 15, 30, 60,150, and 300 min). The complete dataset (three biological replicates) is provided in Supplementary Fig. S2. **a** For insulin, total Akt and pAkt-T308 were monitored by immunoblot. **b** For glucagon, phosphorylation of PKA substrates was monitored by immunoblot. **c**–**e** Quantification of data shown in (**a**); total Akt (**c**), pAkt-T308 (**d**) and ratio pAkt-T308/ total Akt (**e**) were compared between vehicle (HCl) and insulin-treated PCLS; data presented as mean ± SEM. **f** Quantification of data shown in (**b**); phosphorylation of PKA substrates was compared between vehicle (HCl) and glucagon-treated PCLS; data presented as mean ± SEM. **g**–**h** 5 h cumulative net glucose production of PCLS treated with insulin **g** and glucagon **h**; data presented as mean ± SEM. **i** Immunoblotting of PCLS derived from fed mice incubated with WE medium supplemented with DHA and treated with forskolin; phosphorylation of PKA substrates was monitored. The complete dataset (three biological replicates) is provided in Supplementary Fig. S3. **j** Quantification of data shown in (**i**); phosphorylation of PKA substrates was compared between vehicle (DMSO) and forskolin-treated PCLS; data presented as mean ± SEM. **k** 5 h cumulative net glucose production of PCLS treated with forskolin. For all the analyses, vehicle- and hormone-treated groups were compared using two-way ANOVA followed by Tukey multiple comparison test; $^{*}p < 0.05$, vs the corresponding vehicle; data presented as mean ± SEM; $n = 3$ mice per group.

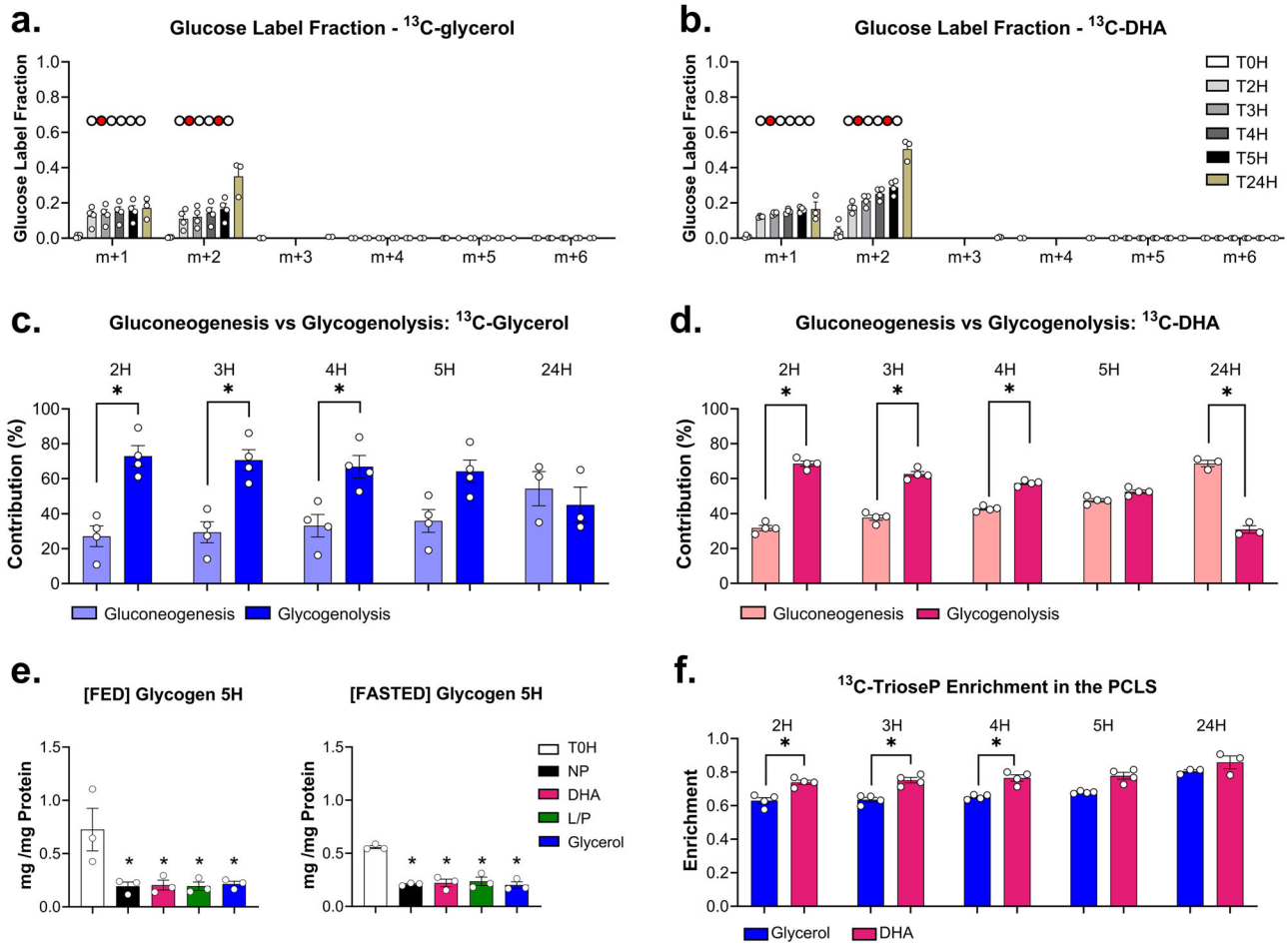

Fig. 4 | Sources of glucose in the PCLS derived from fed mice. Glucose label fraction from PCLS incubated with **a** ^{13}C-glycerol and **b** ^{13}C-DHA for 24 h; Calculated contribution of glycogenolysis and gluconeogenesis in the net glucose production of PCLS incubated with **c** ^{13}C-glycerol and **d** ^{13}C-DHA; **e** Glycogen stores in PCLS derived from fed and fasted mice incubated with WE medium supplemented with DHA, Lactate Pyruvate (L/P), Glycerol for 5 h; *p < 0.05, vs T0H; $n = 3$ mice per group; **f** ^{13}C-TrioseP enrichment in PCLS incubated with either ^{13}C-glycerol (blue) or ^{13}C-DHA (magenta); data presented as mean ± SEM. For (**c**, **d**, **f**) $*p < 0.05$; $n = 3$–4 mice per group.

the loss of SLC37A4 primarily leads to decreased hepatic glucose production, intracellular accumulation of G6P, and as a consequence, enhanced cellular production of lactate and storage of glycogen (Fig. 5a). To test if murine PCLS could mimic this clinical phenotype, they were treated for 5 h with S4048, a pharmacological inhibitor of SLC37A4[26]. In agreement with the clinical phenotype of GSD Ib patients, PCLS derived from both fed and fasted mice showed reduced net glucose production rates (Fig. 5b, c), elevated net lactate production (Fig. 5d, e), and less utilization of glycogen (Fig. 5f, g) upon incubation with S4048. In agreement with earlier observations (Fig. 1), PCLS derived from fasted mice showed a lower net glucose production rate than those of fed mice, which was further decreased by S4048 (Fig. 5c). These results suggest that PCLS can be effectively used to study the acute hepatic GSD Ib human clinical phenotype.

Human PCLS as an ex vivo model to study dysfunctional glucose production

Finally, we questioned if PCLS derived from human liver (hPCLS) could also be used to study (dys)functional glucose production ex vivo. In previous studies, hPCLS were used to evaluate the safety and efficacy of drug candidates[27,28], and to model liver diseases ex vivo (e.g., metabolic dysfunction-associated steatotic liver disease, MASLD)[29–31]. hPCLS derived from two human livers were individually incubated in WE medium up to 5 h, either without or with a gluconeogenic precursor. In both experiments, hPCLS produced glucose in the presence and absence of gluconeogenic substrates (Fig. 6a, b). In contrast to the murine PCLS, however, hPCLS did not exhibit a time-dependent increase in net cumulative glucose production. In hPCLS derived from human liver I, as in murine PCLS, DHA supplementation yielded the highest net cumulative glucose levels of the three precursors (Fig. 6a). In PCLS from both livers, pharmacological inhibition of SLC37A4 by S4048 decreased the net cumulative glucose production (Fig. 6b, c and Supplementary Fig. S4). This was more evident in the PCLS supplemented with DHA, as without precursor the net glucose levels were very low anyway (Fig. 6b, c).

Exceptionally, we had the opportunity to evaluate the net glucose production of hPCLS from one GSD Ia and one Ib patient who underwent liver transplantation. In both cases, the medium glucose levels remained below detection limit, during the entire 5 h of incubation, irrespective of the incubation time and gluconeogenic substrate used (Fig. 6a, three replicates, based on separate incubations of slices derived from the same liver). PCLS from the GSD Ia patient showed low ATP contents (<2 pmol/µg protein) (Supplementary Table S6), below the range considered acceptable for livers from healthy donors[32]. The hepatic mitochondrial oxygen consumption rate in liver mitochondria isolated from the GSD Ia patient was also lower than that of the GSD Ib patient (Supplementary Fig. S5). In both livers, State 4 respiration was low, demonstrating that there was little proton leak, thereby suggesting mitochondrial integrity.

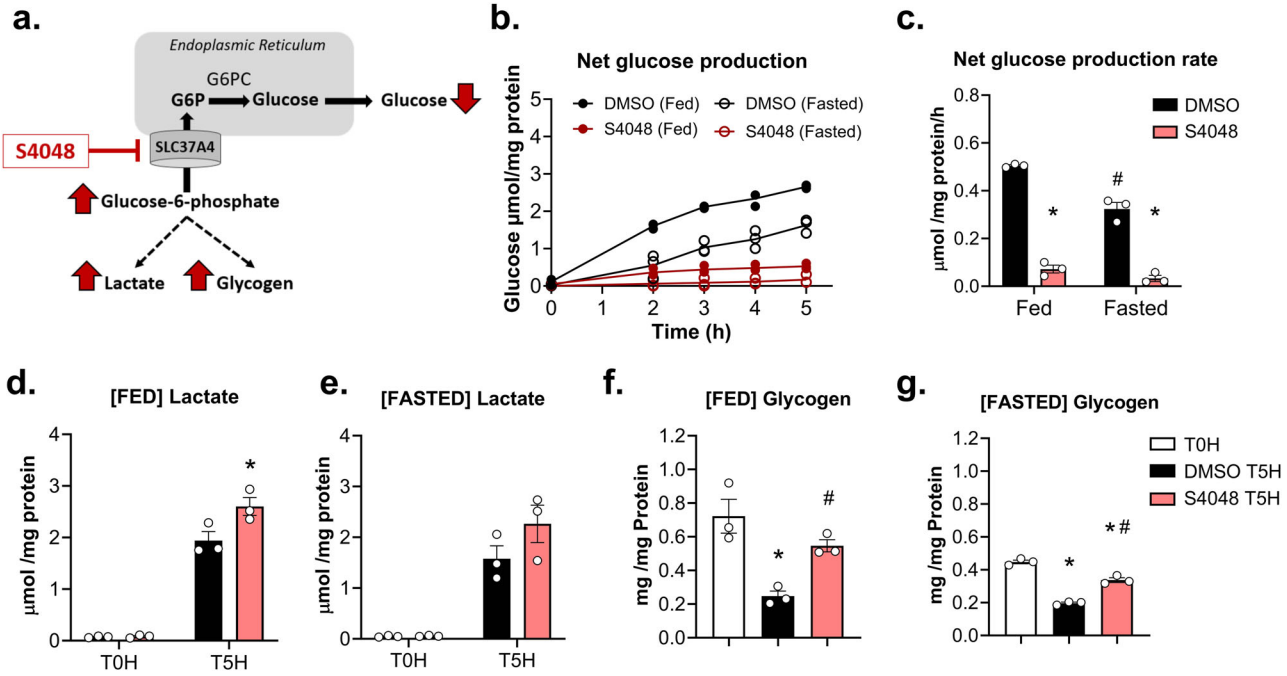

Fig. 5 | PCLS as an ex vivo model of GSD type Ib. a Schematic representation of the mechanism of action and expected effects of S4048, a SLC37A4 inhibitor; **b**–**g** PCLS derived from fed and fasted mice were incubated in WE medium supplemented with DHA plus DMSO (black) or S4048 (red); **b** 5 h net cumulative glucose production of PCLS derived from fed (●) and fasted (○) mice; **c** Net glucose production rate; $^{*}p < 0.05$, vs DMSO group in the same condition; $^{\#}p < 0.05$, vs DMSO group from fed mice; 5 h net cumulative lactate in the medium of PCLS from fed **d** and fasted **e** mice; $^{*}p < 0.05$, vs DMSO; glycogen stores from fed **f** and fasted **g** mice; $^{*}p < 0.05$, vs T0H; $^{\#}p < 0.05$, vs DMSO 5H; data presented as mean ± SEM, $n = 3$ mice per group.

In essence, these results are consistent with the observations made in murine PCLS, illustrating that hPCLS produce glucose ex vivo and can be used to study dysfunctional glucose production in human liver tissue.

Discussion

This study comprehensively and quantitatively analyzed net glucose production rates of PCLS, within the first 24 h of ex vivo culture. For this purpose, PCLS were incubated with commonly used gluconeogenic precursors and the contributions of glycogenolysis and gluconeogenesis to net glucose production were assessed over time. Herein, we show that: (1) net glucose production rates depend on the feeding state at the time of liver tissue collection, with rates being higher in the PCLS from fed than from fasted mice; (2) DHA supplementation to PCLS from fed mice yields the highest net glucose production rates; (3) over 24 h incubation the contribution of glycogenolysis to net glucose production decreases in favor of that of gluconeogenesis (4) murine and human PCLS can be used to model and investigate impaired hepatic glucose production in IEMs, such as GSD Ia and Ib.

In a direct comparison of net glucose production rates among different hepatic in vitro and ex vivo models (Table 1) compiled from the literature, PCLS exhibited the highest rates (Table S2). Based on calculated endogenous glucose production rates, we estimated in vivo total glucose production rate in mice to be 1667 nmol/mg protein/h (Table S1). It is important to note that this value does not only represent the liver, but also includes some contribution from kidney and intestine[33–35]. PCLS exhibited 17% (no precursor) to 32% of this rate under fed conditions (DHA supplementation), whereas immortalized mouse hepatocytes (AML12 cells) line and murine primary hepatocytes recuperated only 3% and 17% of the in vivo glucose production capacity, respectively (Table 1). The type of gluconeogenic precursor and the experimental design (pre-incubation, feeding state of the mouse) significantly affected the rate of glucose production. The difference between mouse PCLS and primary hepatocytes may be explained by the fact that the PCLS contained a substantial amount of glycogen, which was the dominant source of glucose in the first 3–5 h, suggesting that the rate of gluconeogenesis is similar between the two models.

DHA has been broadly used as substrate in studies on hepatic glucose production in vitro[14,36,37] and was recently shown to be a useful tool to study redox-regulation of gluconeogenesis[38,39]. In contrast to DHA, glycerol and L/P are gluconeogenic precursors commonly used in vitro as well as natural in vivo precursors[13,20]. A recent study in murine primary hepatocytes compared single gluconeogenic precursors to precursor mixtures[20]. There, glycerol was the preferred substrate, yielding a dose-dependent and higher culture medium glucose level than L/P after 8 h incubation[20]. Unfortunately, the latter study did not include DHA. Moreover, despite its comprehensive analysis of substrate incorporation into gluconeogenesis and TCA cycle intermediates, it did not quantify the net rate of glucose production nor the relative contributions of glycogenolysis and gluconeogenesis. In agreement with our results in PCLS, DHA also yields the highest rate of net glucose production in most studies with hepatocyte suspensions or primary hepatocytes[36–38,40], with the exception of ref.[39]. This is furthermore in agreement with the higher incorporation of the ^{13}C-label from DHA than from glycerol into both glucose and trioseP (Fig. 4c, d, f). Glucose production from glycerol or lactate depends on the cytosolic NADH/NAD^{+} ratio, whereas DHA bypasses the redox reactions (Fig. 1a)[39]. Therefore, the cytosolic redox state of the hepatocytes is a critical determinant of gluconeogenesis from natural precursors[41,42], but not from DHA. This may suggest that gluconeogenesis in the PCLS and primary hepatocytes is limited by the redox state. Alternatively, the abundance of enzymes required specifically for glycerol and pyruvate/lactate metabolism may be limiting in both models.

Notably, PCLS from fasted mice did not respond to any gluconeogenic precursor (Fig. 1d, f). We initially expected that PCLS derived from fasted mice would exhibit higher glucose production rates than those from fed mice, as fasting drives hepatic glucose production in vivo[43]. The opposite result may be explained by PCLS derived from fasted mice re-using a larger fraction of the produced glucose, thereby lowering the net glucose production rate and minimizing the effect of DHA. The glycogen pool did not

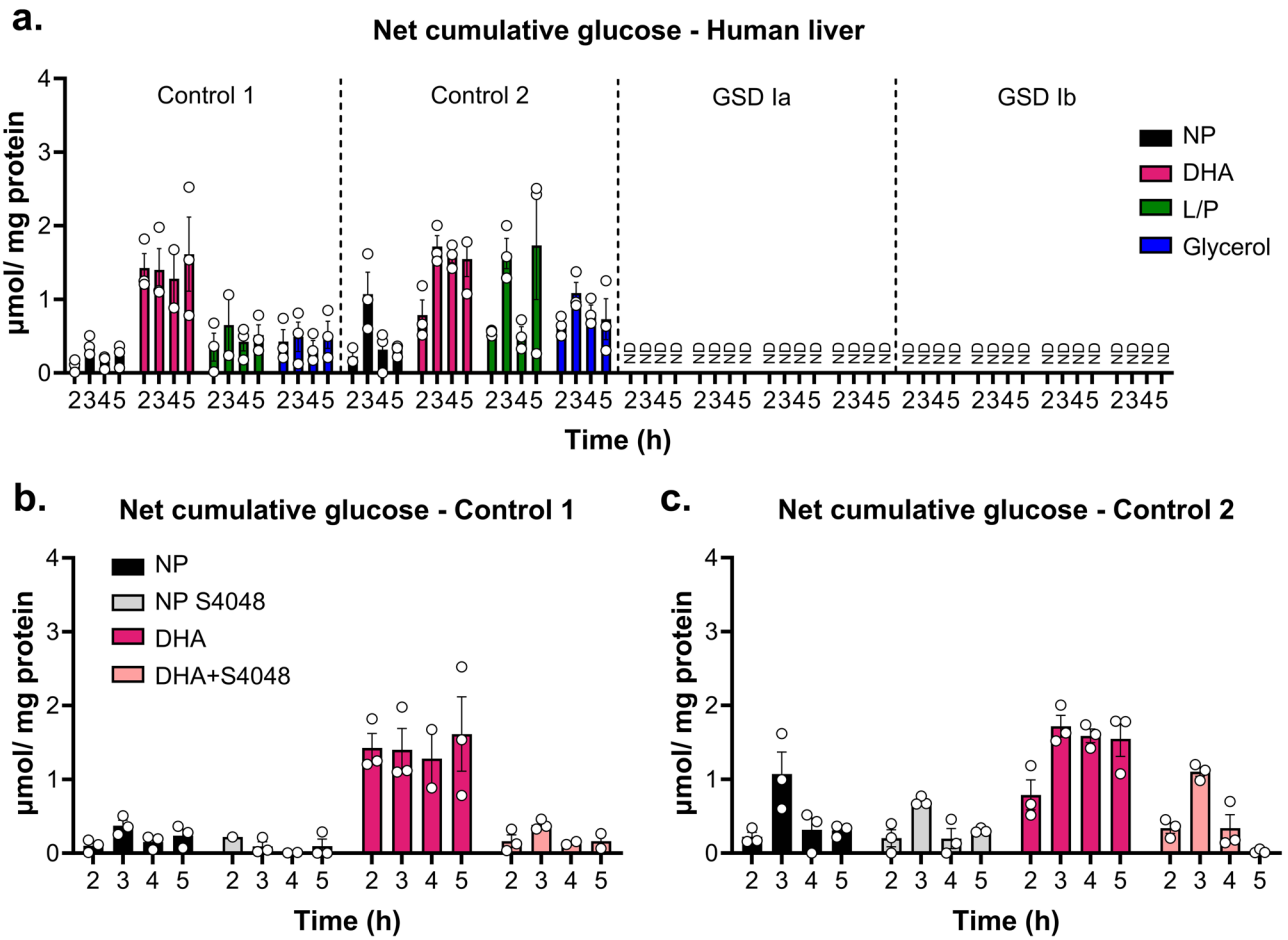

Fig. 6 | Human PCLS produce glucose ex vivo. a PCLS derived from two control human livers, one GSD Ia and one GSD Ib liver were incubated with WE medium without the addition of any precursor NP or supplemented with DHA, Lactate/Pyruvate (L/P), and glycerol for 5 h; **b**–**c** 5 h net cumulative glucose production of PCLS derived from human liver I (**b**) and II (**c**) incubated in WE medium without or with DHA, and plus DMSO (dark color) or S4048 (light color); data presented as mean ± SEM of the three technical replicates. ND means non detectable.

differ substantially between fed and fasted mice (Fig. 4a), hence could not explain the different net glucose production rates observed. Remarkably, the net glucose production was not increased after 24 h of incubation in a high-glucose medium. In fact, the 24 h pre- incubation step even reduced the glucose production rate. Exposure to high glucose has been reported to decrease the glucose 6-phosphatase (G6Pase) level and activity, thus lowering the net glucose production rate[20,43]. In line with this, rat primary hepatocytes showed a 25% reduction in G6Pase activity after 24 h in culture[18,44].

Interestingly, after 24 h incubation in the presence of labeled substrates, the total precursor enrichment was lower than 100% (Fig. 4f). This observation made us question which other sources of non-labeled substrate could be feeding into the TrioseP pool. As outlined in the supplementary text 1, glycogen stored within PCLS would be sufficient and likely represents the primary source of unlabeled glucose in the initial hours. Presumably, after 24 h, the breakdown of remaining unlabeled glycogen may still contribute to the glucose production. Furthermore, we estimated that 0.27 mM of amino acid would be necessary to supply the non-labeled pool. However, amino acid consumption did not reach this extent, which suggests that the amino acids from the medium did not serve as the major substrates for glucose production under these conditions. An alternative source of amino acids would be intracellular degradation of proteins within PCLS. In vivo studies have shown that hepatic autophagy represents an essential source of gluconeogenic precursors in long fasting periods[45–47]. Consistent with an induction of protein degradation, we observed that PCLS from fed mice cultured in the absence of precursors secreted branched-chain amino acids in the medium.

Net glucose production by PCLS did not respond to insulin or glucagon during a long (5 h) incubation (Fig. 2b, c), but was stimulated by forskolin and dibutyryl-cAMP (Fig. 2b–d) and transiently by glucagon (Fig. 3h). The latter compounds increase the intracellular pool of cAMP pool, a second messenger in the glucagon signaling cascade (Fig. 2a). In agreement with this, its downstream target PKA substrate was induced by forskolin (Fig. 3i, j). We confirmed that also glucagon and insulin activated their downstream signaling pathways (Fig. 3a–f), but the effect was only transient in the case of glucagon and attenuated with time in the case of insulin. Non-parenchymal cells have been reported to degrade and internalize insulin and glucagon in vitro. This could reduce their availability and effectiveness over time[48,49] and may explain the lack of response to insulin and glucagon observed in a 5 h incubation. Previously, PCLS have been shown to lower glucose production during shorter (i.e., 20 min) incubations with insulin[15]. In primary rat hepatocytes, 30 and 60 min of incubation with glucagon increased glucose production[50], in agreement with our results. Similarly, mouse primary hepatocytes exhibited a significant decrease in their glycogen content after 30 min incubation with glucagon[13]. Apart from the timing, a critical difference between our study and these previous reports is the multi-cellular composition of PCLS versus primary hepatocytes.

Finally, we tested if human and murine PCLS serve to model major clinical phenotypes of IEMs. For this purpose, we selected GSD type I as a proof of concept, as its primary defects include impaired glucose production

and hepatic glycogen accumulation. The pharmacological inhibition of the glucose 6-phosphate transporter by S4048 markedly reduced glucose production in mouse and human PCLS, indicating the efficacy of this approach to model clinical GSD Ib symptoms. The effect of S4048 in hPCLS was most clear under DHA-supplemented conditions, in which the highest net glucose production rates were measured, consistent with findings in mice. Similarly, net glucose production by hPCLS from a GSD type Ia and a GSD type Ib patient was negligible. The ATP level and mitochondrial oxygen consumption rate were notably lower in the GSD Ia liver than in the GSD Ib liver. As the ATP level is commonly used to assess PCLS viability, one might question the tissue integrity of the GSD Ia liver. However, the oxygen consumption measurements showed coupled respiration, suggesting at least mitochondrial integrity. The fact that respiration was lower in the mitochondria from the Ia patient than in those from the Ib patient may be attributed to mitochondrial dysfunction in GSD Ia, in line with earlier reports[51,52], although we cannot exclude a difference in tissue quality.

A limitation of this study is that only two healthy human livers and two patient livers were included. Nevertheless, particularly the patient livers provided an exceptional opportunity, since GSD I is a rare disease, with a prevalence of 1:100,000 newborns[53,54] and access to human liver depends on liver transplantation. In recent years, living donor transplantations have become feasible for children, making this a realistic treatment option in hepatic inherited metabolic diseases[55,56]. Therefore, glucose production by hPCLS can in principle be measured routinely, when children are transplanted. This information will give an indication of residual G6Pase activity in kidney and intestine, which are not transplanted. Thus, although the availability of human organs and the variation between donors are concerns, these results open the perspective of also using hPCLS for the study of human metabolic diseases. A methodological limitation is that our analysis provides the cumulative contributions of glycogenolysis and gluconeogenesis rather than their relative contributions at a specific time point. To infer the latter a continuous (non-circulating) perfusion system would be required. Moreover, the use of a single-labeled precursor and analysis of label incorporation in only glucose precluded the quantification of cycling between glucose and glucose 6-phosphate (also interpreted as glucose re-uptake) and cycling between glucose 6-phosphate and glycogen. In this respect our approach differs from that of Hellerstein[57,58] and Van Dijk[26], who co-administered multiple labeled substrates and that of Kalemba[20] who analysed the incorporation of label into gluconeogenic intermediates.

In conclusion, this study provides a comprehensive and quantitative analysis of net glucose production in PCLS. This ex vivo system along with the ^{13}C isotope-tracer assay can be used as an effective tool to study the origin of dysfunctional glucose production and glycogen metabolism in IEMs. In addition, this work adds to the growing number of applications for bioreactor-based PCLS systems[30] to investigate liver-centered diseases, such as NAFLD and liver fibrosis[28,59].

Methods

Animals

Male, wild-type C57/BL6 mice (internal breeding line UMCG Central Animal Facility, Groningen, The Netherlands) aged 8–12 weeks were housed at 21 °C and light-controlled (12 h light; from 8.00 a.m. to 8.00 p.m. during summer and from 7.00 a.m. to 7.00 p.m. during winter) conditions, with ad libitum access to water and Chow diet—V1554-70 (Ssniff, Soest, Germany). Mice from the fasted group were overnight fasted for 12 h (21:00–9:00). Drinking water was at all times available. Termination was done via exsanguination under isoflurane/O_2 anesthesia. The liver was harvested, weighed, and stored in ice-cold UW preservation solution (Bridge to Life, #1022622) prior to slicing. We have complied with all relevant ethical regulations for animal use. All animal experiments were approved by the Institutional Animal Care and Use Committee of the University of Groningen (Groningen, The Netherlands) under permit numbers AVD105002015245 and AVD10500202115288, and they are in line with the Guide for the Care and Use of Laboratory Animals.

Human liver biopsy

Human liver tissue was collected from two transplantation donors at the University Medical Center Groningen (UMCG, Netherlands). These livers were used for research purposes after being rejected for transplantation. Informed consent for research purposes was obtained from the donor's relatives. Prior to slicing, hepatic tissue samples were stored in ice-cold UW preservation solution for up to 24 h. Additionally, after obtaining written informed consent, a tissue sample from the liver explant was obtained from a 12-year-old male GSD type Ia and a 11-year-old male GSD type Ib patient who underwent liver transplantation. In both cases, tissue was used for slicing within 3 h after completion of surgery. All experiments were approved by the Research Ethics Committee of UMCG All ethical regulations relevant to human research participants were followed.

Preparation of precision-cut liver slices (PCLS)

Liver biopsy cores were made with a 6 mm biopsy punch (KAI Medical). Murine and human PCLS, of approximately 5 mg and with an estimated thickness of 250–300 µm, were prepared using a Krumdieck Tissue Slicer (Alabama Research and Development), as described elsewhere[32]. Individual slices were kept in culture for up to 24 h in 12-well plates with glucose-free Williams E medium (WE) (US Biological Life Sciences, C17082259) and gentamycin (50 µg/mL, Invitrogen), unless otherwise stated. The plates were kept under a continuous supply of 80% O_2/5% CO_2, shaking at 90 rpm, at 37 °C, as previously described[32].

PCLS culture conditions for net glucose production assays

For time courses of glucose production, individual slices were incubated for up to 24 h in 1.5 mL glucose-free WE medium at pH 7.4 either without any supplementation (no precursor/NP), or supplemented with different gluconeogenic precursors: 10 mM DHA, 20 mM lactate and 2 mM pyruvate (L/P), and 10 mM glycerol (final concentrations) (Fig. 1a, b). These concentrations are in agreement with the literature, in which up to 20 mM of these substrates was used, typically at a lactate to pyruvate ratio of 10–1[20,36–38,40,60]. If not mentioned otherwise, the slices were placed in the aforementioned medium immediately after slicing. Alternatively, the slices were pre-incubated in WE medium supplemented with 11 mM glucose (Gibco, 32551-020) for 24 h after which there was a switch to glucose-free medium (Fig. 1a). To calculate the net glucose production rates, medium samples (100 µL) were collected at 0, 2, 3, 4, 5, and 24 h.

To test if the net glucose production by the PCLS responds to hormone or pharmacological stimulation, the slices were incubated in WE medium either without any supplementation or with 10 mM DHA, plus: (I) insulin (0.1 or 1 µM)[60] (Sigma–Aldrich, I2643), (II) glucagon (0.1 or 1 µM) (Sigma–Aldrich, G2044)[61,62], (III) forskolin (10 or 20 µM) (Tocris Biosciences, 1099)[23], (IV) dibutyryl-cAMP (50–100 µM) (Sigma–Aldrich, 16980-89-5)[23,63]. Insulin and glucagon were both prepared in HCl (17.3 µM final concentrations, which was used as vehicle control). Based on previous reports of hormone degradation by liver tissue[48,49,64], supraphysiological concentrations of insulin and glucagon were used in order to mitigate potential hormone loss during the 5h-incubation protocol, in agreement with earlier studies[61,65].

To mimic GSD Ib, murine and human PCLSs were incubated with the compound S4048 (10 µM) (kindly provided by Sanofi S.A.), a pharmacological inhibitor of the glucose 6-phosphate (G6P) transporter SLC37A4[26]. Its solvent DMSO (0.1% final concentration) was used as vehicle control. In addition, net glucose production by PCLS from GSD Ia and Ib patients were assessed either in the presence of S4048 (10 µM) or DMSO.

ATP quantification

The viability of the slices was assessed by quantification of the intracellular ATP content using a bioluminescence kit (Roche Diagnostics), as described elsewhere[32]. The ATP values were corrected for the protein content, measured according to Lowry (BioRad DC Protein Assay). The slices were considered viable and accepted when their ATP content was equal to or above 2 pmol/ µg protein[32] (Supplementary Tables S3 and S6).

High-resolution respirometry in liver mitochondria isolated from GSD I patient liver biopsies

Mitochondria were isolated from fresh liver tissue biopsies as described elsewhere[66]. Oxygen consumption rates were measured at 37 °C using a two-channel high-resolution Oroboros oxygraph-2k (Oroboros) in MiR05 buffer (110 mM sucrose, 60 mM potassium lactobionate, 20 mM taurine, 20 mM HEPES, 0.5 mM EGTA, 10 mM KH_2PO_4, 3 mM $MgCl_2$, and 1 mg/ml bovine serum albumin, pH7.1)[67]. First, mitochondria were injected into the instrument along with substrates to measure residual oxygen consumption (State 2). The following substrate combinations were used: (I) 2 mM pyruvate and 2 mM malate, (II) 25 µM palmitoyl-carnitine and 2 mM malate, (III) 25 µM palmitoyl-CoA, 2 mM L-carnitine, and 2 mM malate, and (IV) 5 mM glutamate and 2 mM malate. Next, an ADP- generating method was applied to measure maximal coupled respiration (State 3), which consisted of hexokinase (1.5 U/mL), glucose (10 mM), and ATP (1 mM). The basal respiration (State 4) was determined by the subsequent addition of 1.25 µM carboxyatractyloside (CAT) to inhibit ADP/ATP translocase. Finally, uncoupled respiration (State U) was measured after subsequent administration of 1.5 µM carbonyl cyanide p-(trifluoromethoxy) phenylhydrazone (FCCP). DatLab software (Oroboros) was used for data acquisition and analysis. Oxygen consumption rates were normalized to mitochondrial protein, which was quantified using the BCA assay (Thermo Scientific, 23225).

Metabolite analyses in PCLS culture medium

Glucose and lactate concentrations in the medium were enzymatically determined as described elsewhere[68]. The amino acid concentration in the medium was measured by GC/MS at three time points (0, 5, and 24 h), according to Evers[68].

Glycogen measurement

Glycogen content was quantified using an enzymatic assay[69]. Briefly, individual PCLS were incubated with 500 µL 1 M KOH at 90 °C (30 min, 600 rpm). In a new tube, 200 µL 3 M acetic acid was added to 400 µL sample or 400 µL standard, to achieve pH 5.0, and samples were spun down (4 min, 13.523 g, 4 °C) to precipitate the protein. Next, glycogen was broken down into glucose by the addition of 600 µL of amyloglucosidase solution (4.8 units amyloglucosidase in 0.2 M acetate buffer pH 5.6) to 400 µL supernatant of the previous step. Samples were incubated at 37 °C (at least 60 min, 600 rpm). For glucose determination, either 10 µL standard or 50 µL sample was incubated with 1.25 mL or 1.21 mL incubation buffer pH 7.5 (0.3 M triethanolamine, 30 mM $MgSO_4$, 12.6 mM ATP, 1 mM β-NADP.Na_2H), respectively. 7 units of glucose 6-phosphate dehydrogenase (EC 1.1.1.49; Roche, 10737232.001) was added. Background absorbance at 340 nm was measured (A340-1). To start the reaction, 4.4 units of hexokinase (EC 2.7.1.1; Sigma–Aldrich, 11426362001) were added and endpoint absorbance at 340 nm was measured after 5 min (A340-2). The difference between background and endpoint absorption (340-2–A340-1) was used for quantification.

Glucose isotope tracing

PCLS derived from fed mice were incubated for 5 h or 24 h in glucose-free WE medium supplemented with the following gluconeogenic substrates: (1) 10 mM glycerol, (2) 10 mM [2-^{13}C]-glycerol (Sigma–Aldrich, 489484). (3) 10 mM DHA, (4) 10 mM [2-^{13}C]-DHA (Sigma–Aldrich, 767891). In order to obtain a stock solution of 1 M monomeric DHA, 0.1 g 1,3-Dihydroxyacetone-[2-^{13}C] dimer was resuspended in 1.1 mL Milli-Q H2O while rotating overnight at room temperature[70].

From each time point, 100 µL of medium was used for the analysis. The detailed protocol for preparation of glucose penta acetate derivatives from culture medium samples, and their subsequent GC/MS analysis has been described elsewhere[71]. The measured isotopologue distribution (*m*/z 408–414) in glucose derived from samples incubated with the labeled substrate was corrected for the natural abundance of isotopes[72].

One glucose molecule is formed by the combination of two triose phosphates, dihydroxyacetone-phosphate (DHAP) and glyceraldehyde 3-phosphate (GA3P), which are interconvertible. In the following, the DHAP and G3P pool together will be denoted as TrioseP. According to the combination of labeled and non-labeled TrioseP, glucose could be found in three forms: non-labeled (m + 0; *m*/*z* 408), single-labeled (m + 1; *m*/*z* 409), or double-labeled (m + 2; *m*/*z* 410) (Fig. 7). The ^{13}C-labeled TrioseP fraction (to be inferred) is denoted by *p* (Fig. 7). The fraction of glucose derived from glycogen is denoted by F_{Glycogen} and the fraction derived from gluconeogenesis by F_{GNG}. The subfractions $\mathrm{Glucosem}_{+0}$, $\mathrm{Glucosem}_{+1}$ and $\mathrm{Glucosem}_{+2}$ within the gluconeogenesis fraction are denoted by P_0, P_1 and P_2(Fig. 7), respectively, with:

$$P_0 = (1-p)^2 \tag{1}$$

$$P_1 = 2\cdot(p)\cdot(1-p) \tag{2}$$

$$P_2 = p^2 \tag{3}$$

The sum of P_0, P_1, and P_2 is one. Therefore, it can be derived that p equals:

$$p = \frac{2}{P_1/P_2 + 2} \tag{4}$$

The measured sub fractions of $\mathrm{Glucosem}_{+0}$, $\mathrm{Glucosem}_{+1}$, and $\mathrm{Glucosem}_{+2}$ are denoted by Q_0, Q_1, and Q_2, respectively. Since $\mathrm{Glucosem}_{+1}$ and $\mathrm{Glucosem}_{+2}$ are solely generated via gluconeogenesis, the ratio P_1/P_2 equals the measured ratio Q_1/Q_2. Therefore, *p* could be calculated directly from the data, based on:

$$p = \frac{2}{Q_1/Q_2 + 2} \tag{5}$$

Subsequently, P_0, P_1, and P_2 were calculated by substituting *p* in Eqs. 1–3.

The measured fractions Q_0, Q_1, and Q_2 relate to F_{GNG} via:

$$Q_0 = F_{\mathrm{glycogen}} + F_{\mathrm{GNG}}\cdot P_0 = (1 - F_{\mathrm{GNG}}) + F_{\mathrm{GNG}}\cdot P_0 \tag{6}$$

$$Q_1 = F_{\mathrm{GNG}}\cdot P_1 \tag{7}$$

$$Q_2 = F_{\mathrm{GNG}}\cdot P_2 \tag{8}$$

Thus, F_{GNG} and F_{glycogen} were calculated according to:

$$F_{\mathrm{GNG}} = Q_1/P_1 = Q_2/P_2 \tag{9}$$

$$F_{\mathrm{glycogen}} = 1 - F_{\mathrm{GNG}} \tag{10}$$

It should be noted that any cycling of labeled glucose 6-phosphate via glycogen[26] is not accounted in this analysis. Labeled glucose that is incorporated into glycogen escapes our observation, possibly leading to an underestimation of gluconeogenesis. If labeled precursor is first incorporated into glycogen via gluconeogenesis and subsequently released as glucose into the medium, it is interpreted as part of the gluconeogenesis fraction. The strength of the correction for the inferred enrichment of the Triose-P pool is that the calculated gluconeogenesis includes the cumulative contribution of all gluconeogenic contributions, not only that of the labeled precursor.

Tissue lysis and immunoblotting

For each experimental condition, three slices (technical replicates) were pooled in one 1.5 mL tube and 400 µL of radio immunoprecipitation

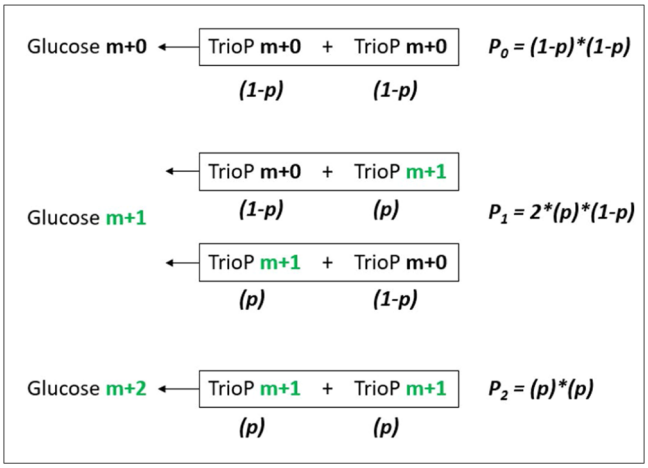

Fig. 7 | ^{13}C-labeled trioseP enrichment in glucose. Calculation of ^{13}C-labeled trioseP enrichment (p) in glucose. Equations 1–3.

assay buffer was added (1% IGEPAL CA-630, 0.1% SDS, and 0.5% sodium deoxycholate in PBS). RIPA buffer was supplemented with Phosphatase Inhibitor Cocktail 2 (Sigma–Aldrich, P5726) and Cocktail 3 (Sigma–Aldrich, P0044) and Complete Protease Inhibitor Cocktail (Sigma–Aldrich, 1186145001). Next, samples were homogenized using a Mini beadbeater (6000 Hz, 45 s, 4 cycles, on ice) (Bertin Technology). Lysates were kept on ice for 15 min and then spun down at maximum speed for 10 min at 4 °C. Protein content was determined using Protein Lowry Assay Kit (BioRad DC Protein Assay). Lysates were adjusted with Laemmli loading buffer (5×: 60 mM Tris-Cl pH 6.8, 10% glycerol, 1% SDS, 0.05% Bromophenol Blue, 1% beta-mercaptoethanol). The protocol followed for immunoblotting has been described elsewhere[73]. Briefly, protein separation was performed in SDS-PAGE 10–14% using a Mini PROTEAN Tetra Vertical Electrophoresis Cell system (Bio-Rad). For western blot, proteins were transferred to a polyvinylidene difluoride membrane (Immobilon®-P, Millipore). The following primary antibodies were used: GAPDH (Abcam, AB8245), Vinculin (Cell Signaling, 4650), Phospho-PKA Substrate (RRXS*/T*) (100G7E) (Cell Signaling, 9624), Akt (pan) (Cell Signaling, 4691), Phospho-Akt (thr308) (Cell Signaling, 2965).

Statistics and reproducibility

Each experiment consisted of at least three biological replicates (PCLS obtained from three different mice). Regarding human PCLS, each experiment consisted of three technical replicates (three PCLS obtained from the same liver biopsy). The results are presented as mean ± standard error of the mean. For the time courses and comparisons between fed and fasted mice, two-way repeated measures ANOVA followed by Dunnett's multiple comparisons test was used. Ordinary one-way ANOVA followed by Tukey's multiple comparison test was used for comparisons between control (e.g., no precursor or vehicle treatment) and treatments (e.g., gluconeogenic substrates, hormones) at a single time point. These analyses were performed using GraphPad Prism version 9.1 for Windows (GraphPad Software). The results were considered statistically significant when the p- value was smaller than 0.05.

Reporting summary

Further information on research design is available in the Nature Portfolio Reporting Summary linked to this article.

Data availability

The numerical source data for the main and Supplementary Figs. are available in the Supplementary Data Files 1 and 2, respectively. The uncropped blots are available in the Supplementary Data file 3. The authors declare that data supporting the findings of this study are available within the manuscript and its supplementary files.

Received: 23 October 2023; Accepted: 14 October 2024;
Published online: 09 November 2024

References

1. Solares, I. et al. Diagnosis and management of inborn errors of metabolism in adult patients in the emergency department. *Diagnostics* **11**, 2148 (2021).
2. Waters, D. et al. Global birth prevalence and mortality from inborn errors of metabolism: a systematic analysis of the evidence. *J. Glob. Health* **8**, 021102 (2018).
3. Ferreira, C. R., Cassiman, D. & Blau, N. Clinical and biochemical footprints of inherited metabolic diseases. II. metabolic liver diseases. *Mol. Genet. Metab.* **127**, 117–121 (2019).
4. Ferreira, C. R. et al. An international classification of inherited metabolic disorders (ICIMD). *J. Inherit. Metab. Dis.* **44**, 164–177 (2021).
5. Agana, M., Frueh, J., Kamboj, M., Patel, D. R. & Kanungo, S. Common metabolic disorder (inborn errors of metabolism) concerns in primary care practice. *Ann. Transl. Med.* **6**, 469–469 (2018).
6. Koeberl, D. D., Kishnani, P. S. & Chen, Y. T. Glycogen storage disease types I and II: treatment updates. *J. Inherit. Metab. Dis.* **30**, 159–164 (2007).
7. Landman, G. W. et al. The relationship between glycaemic control and mortality in patients with type 2 diabetes in general practice (ZODIAC-11). *Br. J. Gen. Pract.* **60**, 172–175 (2010).
8. Ekberg, K. et al. Contributions by kidney and liver to glucose production in the postabsorptive state and after 60 h of fasting. *Diabetes* **48**, 292–298 (1999).
9. Gastaldelli, A., Gaggini, M. & DeFronzo, R. A. Role of adipose tissue insulin resistance in the natural history of type 2 diabetes: results from the san antonio metabolism study. *Diabetes* **66**, 815–822 (2017).
10. Gerich, J. E. Role of the kidney in normal glucose homeostasis and in the hyperglycaemia of diabetes mellitus: therapeutic implications. *Diabet. Med.* **27**, 136–142 (2010).
11. Kaneko, K. et al. The role of kidney in the inter-organ coordination of endogenous glucose production during fasting. *Mol. Metab.* **16**, 203–212 (2018).
12. Magnusson, I., Rothman, D. L., Katz, L. D., Shulman, R. G. & Shulman, G. I. Increased rate of gluconeogenesis in type II diabetes mellitus. A 13C nuclear magnetic resonance study. *J. Clin. Investig.* **90**, 1323–1327 (1992).
13. Nagarajan, S. R. et al. Lipid and glucose metabolism in hepatocyte cell lines and primary mouse hepatocytes: a comprehensive resource for in vitro studies of hepatic metabolism. *Am. J. Physiol. Endocrinol. Metab.* **316**, E578–E589 (2019).
14. Fujiwara, H. et al. Curcumin inhibits glucose production in isolated mice hepatocytes. *Diabetes Res. Clin. Pract.* **80**, 185–191 (2008).
15. Buettner, R. et al. Efficient analysis of hepatic glucose output and insulin action using a liver slice culture system. *Horm. Metab. Res.* **37**, 127–32 (2005).
16. Ross, B. D., Hems, R. & Krebs, H. A. The rate of gluconeogenesis from various precursors in the perfused rat liver. *Biochem. J.* **102**, 942–951 (1967).
17. Argaud, D., Kirby, T. L., Newgard, C. B. & Lange, A. J. Stimulation of glucose-6-phosphatase gene expression by glucose and fructose-2,6-bisphosphate. *J. Biol. Chem.* **272**, 12854–12861 (1997).
18. Gebhardt, R., Bellemann, P. & Mecke, D. Metabolic and enzymatic characteristics of adult rat liver parenchymal cells in non-proliferating primary monolayer cultures. *Exp. Cell Res.* **112**, 431–441 (1978).
19. Han, H. S., Kang, G., Kim, J. S., Choi, B. H. & Koo, S. H. Regulation of glucose metabolism from a liver-centric perspective. *Exp. Mol. Med.* **48**, 1–10 (2016).

20. Kalemba, K. M. et al. Glycerol induces G6pc in primary mouse hepatocytes and is the preferred substrate for gluconeogenesis both in vitro and in vivo. *J. Biol. Chem.* **294**, 18017–18028 (2019).
21. Jiang, G. & Zhang, B. B. Glucagon and regulation of glucose metabolism. *Am. J. Physiol. Metab.* **284**, E671–E678 (2003).
22. Streeper, R. S. et al. A multicomponent insulin response sequence mediates a strong repression of mouse glucose-6-phosphatase gene transcription by insulin. *J. Biol. Chem.* **272**, 11698–11701 (1997).
23. Cullen, K. S., Al-Oanzi, Z. H., O'Harte, F. P. M., Agius, L. & Arden, C. Glucagon induces translocation of glucokinase from the cytoplasm to the nucleus of hepatocytes by transfer between 6-phosphofructo 2-kinase/fructose 2,6-bisphosphatase-2 and the glucokinase regulatory protein. *Biochim. Biophys. Acta* **1843**, 1123–1134 (2014).
24. Yoon, C., Kim, D., Lim, J. H. & Lee, G. M. Forskolin increases cAMP levels and enhances recombinant antibody production in CHO cell cultures. *Biotechnol. J*. **15**, 2000264 (2020).
25. Parikh N.S., Ahlawat, R. *Glycogen Storage Disease Type I* (StatPearls Publishing, accessed 22 January 2024). https://www.ncbi.nlm.nih.gov/books/NBK534196/
26. van Dijk, T. H. et al. Acute inhibition of hepatic glucose-6-phosphatase does not affect gluconeogenesis but directs gluconeogenic flux toward glycogen in fasted rats. *J. Biol. Chem.* **276**, 25727–25735 (2001).
27. Hadi, M. et al. Human precision-cut liver slices as an ex vivo model to study idiosyncratic drug-induced liver injury. *Chem. Res. Toxicol.* **26**, 710–720 (2013).
28. Westra, I. M. et al. Human precision-cut liver slices as a model to test antifibrotic drugs in the early onset of liver fibrosis. *Toxicol. in Vitro* **35**, 77–85 (2016).
29. Palma, E., Doornebal, E. J. & Chokshi, S. Precision-cut liver slices: a versatile tool to advance liver research. *Hepatol. Int.* **13**, 51–57 (2019).
30. Paish, H. L. et al. A bioreactor technology for modeling fibrosis in human and rodent precision-cut liver slices. *Hepatology* **70**, 1377–1391 (2019).
31. Dewyse, L. et al. Improved precision-cut liver slice cultures for testing drug-induced liver fibrosis. *Front. Med*. **9**, 862185 (2022).
32. de Graaf, I. A. M. et al. Preparation and incubation of precision-cut liver and intestinal slices for application in drug metabolism and toxicity studies. *Nat. Protoc.* **5**, 1540–1551 (2010).
33. Hijmans, B. S. et al. Hepatocytes contribute to residual glucose production in a mouse model for glycogen storage disease type Ia. *Hepatology* **66**, 2042–2054 (2017).
34. Oosterveer, M. H. et al. Fenofibrate simultaneously induces hepatic fatty acid oxidation, synthesis, and elongation in mice. *J. Biol. Chem.* **284**, 34036–34044 (2009).
35. Bandsma, R. H. J. et al. Hepatic de novo synthesis of glucose 6-phosphate is not affected in peroxisome proliferator-activated receptor α-deficient mice but is preferentially directed toward hepatic glycogen stores after a short term fast. *J. Biol. Chem.* **279**, 8930–8937 (2004).
36. Rigoulet, M., Leverve, X. M., Plomp, P. J. & Meijer, A. J. Stimulation by glucose of gluconeogenesis in hepatocytes isolated from starved rats. *Biochem. J.* **245**, 661–8 (1987).
37. Hue, L. & Bartrons, R. Role of fructose 2,6-bisphosphate in the control by glucagon of gluconeogenesis from various precursors in isolated rat hepatocytes. *Biochem. J.* **218**, 165–70 (1984).
38. Alshawi, A. & Agius, L. Low metformin causes a more oxidized mitochondrial NADH/NAD redox state in hepatocytes and inhibits gluconeogenesis by a redox-independent mechanism. *J. Biol. Chem.* **294**, 2839–2853 (2019).
39. Madiraju, A. K. et al. Metformin inhibits gluconeogenesis via a redox-dependent mechanism in vivo. *Nat. Med.* **24**, 1384–1394 (2018).
40. Soler, C. & Soley, M. Rapid and delayed effects of epidermal growth factor on gluconeogenesis. *Biochem. J.* **294**, 865–72 (1993).
41. LaMoia, T. E. et al. Metformin, phenformin, and galegine inhibit complex IV activity and reduce glycerol-derived gluconeogenesis. *Proc. Natl. Acad. Sci. USA* **119**, e2122287119 (2022).
42. Yoon, J. C. et al. Control of hepatic gluconeogenesis through the transcriptional coactivator PGC-1. *Nature* **413**, 131–138 (2001).
43. Arden, C. et al. Elevated glucose represses liver glucokinase and induces its regulatory protein to safeguard hepatic phosphate homeostasis. *Diabetes* **60**, 3110–3120 (2011).
44. Spagnoli, D., Dobrosielski-Vergona, K. & Widnell, C. C. Effects of hormones on the activity of glucose-6-phosphatase in primary cultures of rat hepatocytes. *Arch. Biochem. Biophys.* **226**, 182–189 (1983).
45. Ezaki, J. et al. Liver autophagy contributes to the maintenance of blood glucose and amino acid levels. *Autophagy* **7**, 727–736 (2011).
46. Kotoulas, O. B., Kalamidas, S. A. & Kondomerkos, D. J. Glycogen autophagy in glucose homeostasis. *Pathol. Res. Pract.* **202**, 631–8 (2006).
47. Toledo, M. et al. Autophagy regulates the liver clock and glucose metabolism by degrading CRY1. *Cell Metab.* **28**, 268–281.e4 (2018).
48. Watanabe, J., Kanai, K. & Kanamura, S. Glucagon receptors in endothelial and Kupffer cells of mouse liver. *J. Histochem. Cytochem.* **36**, 1081–1089 (1988).
49. Kolaczynski, J. W., Carter, R., Soprano, K. J., Moscicki, R. & Boden, G. Insulin binding and degradation by rat liver Kupffer and endothelial cells. *Metabolism* **42**, 477–481 (1993).
50. Farghali, H. et al. Glucose release as a response to glucagon in rat hepatocyte culture: involvement of NO signaling. *Physiol. Res*. 569–575. https://doi.org/10.33549/physiolres.931232 (2008).
51. Farah, B. L. et al. Induction of autophagy improves hepatic lipid metabolism in glucose-6-phosphatase deficiency. *J. Hepatol.* **64**, 370–379 (2016).
52. Cho, J., Kim, G., Mansfield, B. C. & Chou, J. Y. Sirtuin signaling controls mitochondrial function in glycogen storage disease type Ia. *J. Inherit. Metab. Dis.* **41**, 997–1006 (2018).
53. Bali, D.S., El-Gharbawy, A., Austin, S., Pendyal S., Kishani, S. P. *Glycogen Storage Disease Type I* (University of Washington, accessed 11 July 2024). https://www.ncbi.nlm.nih.gov/books/NBK1312/
54. Kishnani, P. S. et al. Diagnosis and management of glycogen storage disease type I: a practice guideline of the American College of Medical Genetics and Genomics. *Genet. Med.* **16**, e1 (2014).
55. Vimalesvaran, S. & Dhawan, A. Liver transplantation for pediatric inherited metabolic liver diseases. *World J. Hepatol.* **13**, 1351–1366 (2021).
56. Sood, V., Squires, J. E., Mazariegos, G. V., Vockley, J. & McKiernan, P. J. Living Related Liver Transplantation for Metabolic Liver Diseases in Children. *J. Pediatr. Gastroenterol. Nutr.* **72**, 11–17 (2021).
57. Hellerstein, M. K. et al. Hepatic gluconeogenic fluxes and glycogen turnover during fasting in humans. A stable isotope study. *J. Clin. Invest.* **100**, 1305–19 (1997).
58. Neese, R. A. et al. Gluconeogenesis and intrahepatic triose phosphate flux in response to fasting or substrate loads. Application of the mass isotopomer distribution analysis technique with testing of assumptions and potential problems. *J. Biol. Chem.* **270**, 14452–66 (1995).
59. Prins, G. H. et al. The effects of butyrate on induced metabolic-associated fatty liver disease in precision-cut liver slices. *Nutrients* **13**, 4203 (2021).
60. Aji, G. et al. Regulation of hepatic insulin signaling and glucose homeostasis by sphingosine kinase 2. *Proc. Natl. Acad. Sci. USA* **117**, 24434–24442 (2020).
61. Mckee, R. L. et al. Perifused precision-cut liver slice system for the study of hormone-regulated hepatic glucose metabolism. *J. Pharmacol. Methods* **19**, 339–354 (1988).

62. Zhang, W.-S. et al. Inactivation of NF-κB2 (p52) restrains hepatic glucagon response via preserving PDE4B induction. *Nat. Commun.* **10**, 4303 (2019).
63. Arden, C. et al. Fructose 2,6-bisphosphate is essential for glucose-regulated gene transcription of glucose-6-phosphatase and other ChREBP target genes in hepatocytes. *Biochem. J.* **443**, 111–123 (2012).
64. Antoniello, S. et al. Insulin and glucagon degradation in liver are not affected by hepatic cirrhosis. *Clin. Chim. Acta* **183**, 343–350 (1989).
65. Smith, P. F. et al. Maintenance of adult rat liver slices in dynamic organ culture. *In Vitro Cell. Dev. Biol.* **22**, 706–12 (1986).
66. Mildaziene, V. Multiple effects of 2,2′,5,5′-tetrachlorobiphenyl on oxidative phosphorylation in rat liver mitochondria. *Toxicol. Sci.* **65**, 220–227 (2002).
67. Martines, A. C. M. F. et al. Transcriptome analysis suggests a compensatory role of the cofactors coenzyme A and NAD+ in medium-chain acyl-CoA dehydrogenase knockout mice. *Sci. Rep.* **9**, 1–11 (2019).
68. Evers, B. et al. Simultaneous quantification of the concentration and carbon isotopologue distribution of polar metabolites in a single analysis by gas chromatography and mass spectrometry. *Anal. Chem.* **93**, 8248–8256 (2021).
69. Bergmeyer, H.U., Gawehn, K. *Principles of enzymatic analysis*. (Verlag Chemie, 1978).
70. Belfleur, L., Sonavane, M., Hernandez, A., Gassman, N. R. & Migaud, M. E. Solution chemistry of dihydroxyacetone and synthesis of monomeric dihydroxyacetone. *Chem. Res. Toxicol.* **35**, 616–625 (2022).
71. van Dijk, T. H. et al. A novel approach to monitor glucose metabolism using stable isotopically labelled glucose in longitudinal studies in mice. *Lab. Anim.* **47**, 79–88 (2013).
72. Vieira-Lara, M. A. et al. Age and diet modulate the insulin-sensitizing effects of exercise: a tracer-based oral glucose tolerance test. *Diabetes* https://doi.org/10.2337/db220746 (2023).
73. Heberle, A. M. et al. The PI3K and MAPK/p38 pathways control stress granule assembly in a hierarchical manner. *Life Sci. Alliance* **2**, e201800257 (2019).
74. Rothman, D. L., Magnusson, I., Katz, L. D., Shulman, R. G. & Shulman, G. I. Quantitation of hepatic glycogenolysis and gluconeogenesis in fasting humans with ^{13}C NMR. *Science* **254**, 573–576 (1991).

Acknowledgements

This project is supported by European Union's Horizon 2020 research and innovation program under the Marie Skłodowska-Curie Actions PoLiMeR Innovative Training Network (Grant Agreement No 812616) and a grant from Stichting De Cock–Hadders. E.B.H. is funded by the University Medical Center Groningen. We thank Mitchel Ruigrok, Yvette Jansen and Hermien Hartog for excellent technical assistance and Sanofi for kindly providing S4048.

Author contributions

K.A.K., L.A.K., and E.B.M. took care of designing and performing the experiments, generating the data, and interpreting the data. K.A.K. and L.A.K. wrote the manuscript. M.L.M., A.G., and D.O. contributed to the slicing and GC/MS tracer analysis. T.B. performed the glycogen analyses. T.G.J.D., A.B.S., V.E.M., and R.J.O., contributed with the human GSD I liver samples and clinical interpretation. K.V.E., P.O., B.M.B., M.H.O. designed the experiments, hypothesized and helped in drafting the manuscript. All authors commented on the text.

Competing interests

The authors declare no competing interests.

Additional information

Supplementary information The online version contains supplementary material available at https://doi.org/10.1038/s42003-024-07070-z.

Correspondence and requests for materials should be addressed to Barbara M. Bakker or Maaike H. Oosterveer.

Peer review information *Communications Biology* thanks Loranne Agius, Rui de Carvalho and Felix Westcott for their contribution to the peer review of this work. Primary Handling Editors: Ngan Huang and Dario Ummarino. A peer review file is available.